

NICST Internal Memo

Date: October 21, 2008

From: J McIntire, C. Pan, and S. Xiong

To: Bruce Guenther, Jim Butler, Jack Xiong

Subject: Cold Plateau RC-05 Part 1 Radiometric Sensitivity for VIIRS EDU

References:

- [1] NICST_MEMO_08_035, "Updated Analysis Results for VIIRS EDU RC-05 Part 1, Cold Plateau," J. McIntire, C. Pan, and S. Xiong, October 14, 2008.
- [2] NICST_REPORT_06_003, 'Preliminary analysis report of EDU TV cold plateau RC-05 Part 1 (22V) radiometric characterization for Thermal Emissive Bands (TEB),' July 12, 2006.
- [3] NICST_REPORT_06_005, 'Preliminary analysis report of VIIRS EDU RC-05 Part 1 in TV at Cold Plateau for all Three Voltage Levels,' July 14, 2006.
- [4] NICST_REPORT_06_025, 'Radiometric Characterization Report of EDU RC-05 Part1 Using BCS at Hot Plateau (28V) and Comparison with Cold & Nominal,' December 13, 2006.
- [5] Y21901, 'VIIRS Test Analysis report for RC-05, Part 1 Bands M12-M16, I4-I5,' Mina Mitani and Heidi Warner, January 17, 2007.
- [6] 'Sensor Performance Verification Plan,' PVP154640-101.
- [7] NICST_MEMO_08_025, "Radiometric Sensitivity of the VIIRS EDU Sensor Determined from the RC-05 Part 1 Test (Nominal Plateau at 28V)," J. McIntire, C. Pan, and S. Xiong, July 10, 2008.
- [8] 'Performance Specification Sensor Specification,' ps154640-101_c.
- [9] NICST_MEMO_08_035, 'Analysis Results for VIIRS EDU RC-05 Parts 1 and 2, Cold Plateau,' J. McIntire, C. Pan, and S. Xiong, October 14, 2008.

1. Introduction

The VIIRS EDU RC-05 test was designed in part to analyze the radiometric sensitivity of the TEB in a near space-like environment using the Blackbody Calibration Source (BCS). This work will focus on the Cold Plateau of RC-05 as an update to previous work [1-4] and as a comparison to other groups published work [5].

Table 1 lists the relevant UAIDs along with their corresponding BCS temperatures for the three BUS voltages of the Cold Plateau. The BCS source was located in the last collect window, and the Space View Source (SVS) was positioned in the Space View (SV) port. Note that only M13 high gain (hg) is considered in this work. The VIIRS sensor was operated in diagnostic mode and each collect contains 100 scans. The general outline of the methodology used in this work follows from [6] with some modifications.

2. Data Processing

The data processing and algorithms used here were described in detail in [7], and as a result, are not repeated here. However, the following modifications have been made:

- 1) The background subtracted source radiances are converted from f9 to f6 by

$$\Delta L_{f6} = \Delta L_{f9} \left(\frac{6}{9} \right)^2. \quad (1)$$

Thus, all the calculations and results presented here are for f6. In addition, the specifications compared to in this work were written assuming f6.

- 2) The subsamples for the I bands are now labeled 1 for the first subsample and 2 for the second subsample.

3. Analysis

In Table 2, the SNR at L_{TYP} are listed for each of the BUS voltages in the Cold Plateau and averaged over both detectors and subsamples for HAM A. The published Raytheon results are also included for comparison [5], except for bands M15, M16A, and M16B. For these bands, L_{TYP} lies outside of the range of measured values (note that while T_{TYP} is within the measured range, scaling the background subtracted radiance to f6 results in L_{TYP} outside the measured range). As a result, the SNR and NEdT at L_{TYP} were determined by extrapolating beyond the measured range. Although the function used to model the SNR is nonlinear, this extrapolation is not that different from a straight line fit to the data at L_{TYP} for these bands. Raytheon did not compare to L_{TYP} for these three bands; instead they evaluated the SNR and NEdT at $T=340$ K (a scene temperature just inside the measured range). Consequently, the Raytheon results are considerably smaller for these bands.

The NEdT at L_{TYP} , averaged over detectors and subsamples, are given in Table 3 for each band and voltage. SRV0053 requires that the NEdT at L_{TYP} be less than the values listed in Table 3 for each band [8]. All the averaged NEdT at L_{TYP} meet the requirement.

The variation in the averaged SNR and NEdT at L_{TYP} over voltage with respect to 28V is small (less than 3%). The exceptions are bands I4 and M15. As described above, the SNR and NEdT at L_{TYP} were extrapolated outside the measured range for some bands; M15 was extrapolated farther than either M16A or M16B, and as a result, more error is introduced into the SNR and NEdT at L_{TYP} . The percent difference from 28V is as high as 10% for M15. For I4, there is as high as 25% variation with respect to 28V. This is the result of an OOF data point at the low end of the dynamic range (BCS temperature of 230 K). Note that the variation between 22V and 34V for I4 is only 1%. This OOF data was discussed in [9].

The SNR at L_{TYP} are listed for each individual detector in Tables 4 – 6 for 22V, 28V, and 34V, respectively. Detectors considered to have low SNR at L_{TYP} are marked in green. For 22V these detectors are: band I5, detectors 6, 8, and 15; band M12, detectors 12, 15, and 16; band M14, detector 10; and band M15, detector 16. For 28V and 34V, the same

detectors are marked (except band M15, detector 16 is no longer marked and band I5, detector 29 is). The SNR as a function of ΔL_{BCS} is shown in Figures 1 – 6 for each band and voltage along with its corresponding fractional fitting residual ([SNR - f(ΔL_{BCS})] / SNR). The dashed green and blue lines represent L_{MIN} and L_{TYP} , respectively. Figures 7 – 9 show the detector variation in SNR at L_{TYP} for all bands and voltages measured during the Cold Plateau. The detectors highlighted in Tables 4 – 6 are also circled in Figures 1 – 9.

In Tables 7 – 9, NEdT at L_{TYP} for every detector is listed for the three voltages. The only detector that fails the requirement is detector 10 in band M14 at 34V (marked in red). The NEdT versus ΔL_{BCS} is graphed for each band in Figures 10 – 12 for 22V, 28V, and 34V, respectively. Figures 13 – 15 show the NEdT at L_{TYP} as a function of detector for the three voltages. Band M14, detector 10 is OOF for all voltages, but only fails the specification at 34V.

Detector 10 for band M14 shows a large standard deviation for each individual sample as a function of scans (at least twice the standard deviations of other detectors in M14). This indicates a larger variation with respect to time. The standard deviations of this detector for each individual scan as a function of sample is also roughly twice the standard deviations of other detectors in M14, which is indicative of larger spatial variation for detector 10. As a result of the spatial and temporal variations, the SNR is low and OOF and the NEdT is high and OOF for this detector. Thus, we conclude that detector 10 for band M14 is noisy.

The detectors highlighted in Tables 4 – 6 (except M14 detector 10) all have large standard deviations, usually about 50% higher than other detectors in the respective bands. However, these detectors exhibit NEdT at L_{TYP} that are comparable to other detectors in the respective bands.

4. Summary

- NEdT at L_{TYP} meet the requirement for all bands and detectors, with the exception of detector 10 in band M14.
- SNR at L_{TYP} are in good agreement with the published findings of Raytheon [4], except bands M15, M16A, and M16B. Different temperatures were used for NICST (T_{TYP}) and Raytheon ($T=340$ K).
- Variation over voltage with respect to 28V is small (less than 3%) for both SNR and NEdT at L_{TYP} . The exceptions are I4 and M15.
- The following detectors exhibit low SNR for at least one voltage: band I5, detectors 6, 8, 15, and 29; band M12, detectors 12, 15, and 16; band M14, detector 10; and band M15, detector 16.
- Detector 10 for band M14 is noisy.

Acknowledgement

The sensor test data used in this document was provided by the SBRS testing team. Approaches for data acquisition and data reductions, as well as data extraction tools were also provided by the SBRS. We would like to thank the SBRS team for their support. The data analysis tools were developed by the NICST team, and we would like to extend our gratitude for their valued assistance.

Table 1: EDU RC-05 Part 1 UAIDs for the Cold Plateau with corresponding BCS and TMC temperatures.

22V			28V			34V	
UAID	BCS Temp (K)	TMC Temp (K)	UAID	BCS Temp (K)	TMC Temp (K)	UAID	BCS Temp (K)
2002076	246.8	~	2002196	190.0	~	2002242	246.9
2002077	261.7	~	2002197	210.1	~	2002243	277.8
2002078	277.6	~	2002198	229.8	~	2002244	307.3
2002079	291.6	~	2002199	246.7	~	2002245	332.3
2002080	306.9	~	2002200	261.8	~	2002246	345.1
2002081	321.3	~	2002201	277.8	~		
2002082	332.4	~	2002202	291.8	~		
2002083	340.0	~	2002204	307.4	~		
2002084	345.1	~	2002205	321.3	~		
			2002206	332.4	~		
			2002207	340.0	~		
			2002208	345.1	~		

Table 2: Detector averaged SNR at L_{TYP} (HAM side A).

Band	Cold Plateau 22V		Cold Plateau 28V		Cold Plateau 34V	
	Raytheon [5]	NICST	Raytheon [5]	NICST	Raytheon [5]	NICST
I4	54.7	58.85	54.7	47.12	53.9	58.34
I5	85.4	93.36	84.8	93.11	86.1	93.24
M12	212	217.8	213	219.9	208	219.7
M13 hg	714	684.8	723	690.7	704	677.8
M14	913	1053	903	1055	920	1064
M15	2224	3081	2225	3364	2258	3219
M16A	1622	2351	1614	2354	1646	2297
M16B	1596	2391	1577	2294	1601	2281

Table 3: Detector averaged NEdT at L_{TYP} (HAM side A).

Band	T _{TYP}	NEdT at T _{TYP} [8]	Cold Plateau 22V	Cold Plateau 28V	Cold Plateau 34V
I4	270	2.500	0.336	0.419	0.339
I5	210	1.500	0.380	0.381	0.380
M12	270	0.396	0.0937	0.0927	0.0929
M13 hg	300	0.107	0.0372	0.0369	0.0377
M14	270	0.091	0.0431	0.0431	0.0429
M15	300	0.070	0.0222	0.0203	0.0210
M16A	300	0.072	0.0319	0.0317	0.0325
M16B	300	0.072	0.0316	0.0325	0.0326

Table 4: Cold Plateau (22V) SNR at L_{TYP} for each band and detector (HAM side A).

Detector	I4	I5	M12	M13 hg	M14	M15	M16A	M16B
1	56.10	100.9	241.3	724.3	1118	3308	2189	2451
2	55.22	92.08	236.9	676.3	1120	2809	2523	2470
3	56.35	101.7	241.1	683.1	1084	3922	2362	2551
4	56.70	97.10	245.9	588.3	1043	3225	2073	2193
5	57.84	91.54	239.5	703.7	950.5	2810	2644	2758
6	58.34	70.49	230.8	692.9	1204	2964	2441	1606
7	59.38	95.38	248.1	714.2	1033	2965	2029	1967
8	58.08	71.53	240.6	652.7	1097	2947	2722	2475
9	60.71	95.85	240.5	674.1	1047	3008	2237	2803
10	60.18	102.1	230.3	684.7	494.7	3377	2339	2286
11	59.82	91.34	221.7	725.9	1170	3081	2462	2668
12	59.41	104.3	118.8	681.8	1264	3103	2824	2529
13	59.36	96.06	199.1	706.0	1272	3007	2609	2665
14	59.59	100.4	217.3	684.6	1047	3549	1874	1989
15	60.31	70.04	158.4	702.1	1012	3440	2002	2663
16	59.78	103.8	173.6	661.9	890	1777	2285	2188
17	60.23	104.0	~	~	~	~	~	~
18	62.14	87.32	~	~	~	~	~	~
19	60.24	102.4	~	~	~	~	~	~
20	60.00	102.0	~	~	~	~	~	~
21	61.71	102.6	~	~	~	~	~	~
22	58.40	91.11	~	~	~	~	~	~
23	58.28	97.78	~	~	~	~	~	~
24	58.84	82.26	~	~	~	~	~	~
25	59.21	96.08	~	~	~	~	~	~
26	57.29	93.11	~	~	~	~	~	~
27	59.41	92.62	~	~	~	~	~	~
28	58.04	95.56	~	~	~	~	~	~
29	59.68	82.18	~	~	~	~	~	~
30	57.77	92.85	~	~	~	~	~	~
31	57.40	91.57	~	~	~	~	~	~
32	57.26	89.22	~	~	~	~	~	~

Table 5: Cold Plateau (28V) SNR at L_{TYP} for each band and detector (HAM side A).

Detector	I4	I5	M12	M13 hg	M14	M15	M16A	M16B
1	45.60	102.7	238.8	702.0	1201	3015	2000	2425
2	44.82	89.91	248.9	725.6	1098	3591	2320	2376
3	45.44	101.7	241.1	714.6	1079	4189	2703	2229
4	45.78	99.31	238.6	603.8	1075	3728	2025	2119
5	46.43	90.89	241.2	740.9	940.5	4365	2766	2469
6	46.59	74.28	240.4	666.4	1191	3411	2473	1982
7	47.04	94.93	247.5	712.3	1051	3004	2708	2346
8	46.92	66.99	245.8	677.2	1103	3083	2666	2313
9	48.42	96.49	242.5	722.7	1028	3082	2356	2523
10	48.23	99.74	237.4	708.0	481.0	2804	2248	1819
11	47.68	92.77	224.0	695.5	1168	2683	2160	2341
12	47.74	105.6	122.5	677.9	1255	2979	2253	2404
13	47.70	97.54	200.0	709.0	1269	3263	2386	2333
14	48.19	99.25	217.8	647.4	1037	4674	2082	1964
15	48.21	74.53	158.0	680.7	991.6	3051	2428	2685
16	47.67	104.1	174.3	666.8	919.3	2898	2087	2377
17	48.16	103.5	~	~	~	~	~	~
18	49.19	86.78	~	~	~	~	~	~
19	48.38	101.8	~	~	~	~	~	~
20	48.23	100.8	~	~	~	~	~	~
21	48.27	101.7	~	~	~	~	~	~
22	46.72	90.61	~	~	~	~	~	~
23	46.59	96.08	~	~	~	~	~	~
24	46.99	84.71	~	~	~	~	~	~
25	47.05	97.50	~	~	~	~	~	~
26	46.11	92.47	~	~	~	~	~	~
27	47.44	88.56	~	~	~	~	~	~
28	46.66	97.20	~	~	~	~	~	~
29	47.20	75.17	~	~	~	~	~	~
30	46.40	89.60	~	~	~	~	~	~
31	45.70	92.84	~	~	~	~	~	~
32	46.41	89.31	~	~	~	~	~	~

Table 6: Cold Plateau (34V) SNR at L_{TYP} for each band and detector (HAM side A).

Detector	I4	I5	M12	M13 hg	M14	M15	M16A	M16B
1	56.31	103.3	234.7	655.9	1187	3102	1883	2309
2	54.66	90.81	244.7	729.5	1117	3126	2245	2281
3	55.69	104.9	251.7	680.7	1113	3395	2465	2253
4	55.91	98.24	237.6	572.6	1086	2784	2025	2209
5	56.69	93.40	242.7	690.6	940.7	2815	2530	2220
6	57.65	71.41	233.8	722.1	1254	3513	2525	2121
7	59.07	95.11	242.9	723.8	1055	3366	2003	2735
8	56.78	78.02	247.2	667.0	1117	3500	2499	2573
9	60.19	90.98	238.4	680.1	1090	2673	2315	2185
10	60.17	99.72	238.2	687.7	469.2	3132	2207	2156
11	58.82	89.88	218.9	701.9	1212	2670	2160	2270
12	59.10	103.5	119.9	711.8	1239	3597	2599	2195
13	60.25	95.55	200.9	688.6	1206	3820	2583	2175
14	59.69	98.75	232.1	620.0	1046	3492	1954	2153
15	59.77	70.40	159.3	697.4	981.0	2591	2318	2551
16	58.85	103.6	172.7	614.4	907.5	3935	2444	2110
17	60.21	102.3	~	~	~	~	~	~
18	61.61	88.43	~	~	~	~	~	~
19	59.76	104.3	~	~	~	~	~	~
20	59.30	100.5	~	~	~	~	~	~
21	60.52	99.86	~	~	~	~	~	~
22	57.76	91.50	~	~	~	~	~	~
23	57.86	99.30	~	~	~	~	~	~
24	58.33	82.49	~	~	~	~	~	~
25	58.50	97.94	~	~	~	~	~	~
26	56.66	92.65	~	~	~	~	~	~
27	59.46	93.04	~	~	~	~	~	~
28	57.50	96.00	~	~	~	~	~	~
29	59.06	73.09	~	~	~	~	~	~
30	57.15	92.90	~	~	~	~	~	~
31	56.60	90.48	~	~	~	~	~	~
32	56.96	91.16	~	~	~	~	~	~

Table 7: Cold Plateau (22V) NEdT at L_{TYP} for each band and detector (HAM side A).

Detector	I4	I5	M12	M13 hg	M14	M15	M16A	M16B
1	0.352	0.347	0.0813	0.0351	0.0387	0.0201	0.0338	0.0301
2	0.357	0.381	0.0828	0.0376	0.0387	0.0237	0.0293	0.0299
3	0.350	0.345	0.0814	0.0372	0.0400	0.0170	0.0313	0.0290
4	0.348	0.361	0.0798	0.0432	0.0415	0.0207	0.0356	0.0337
5	0.341	0.383	0.0819	0.0361	0.0456	0.0237	0.0280	0.0268
6	0.338	0.497	0.0850	0.0367	0.0360	0.0225	0.0303	0.0460
7	0.332	0.367	0.0791	0.0356	0.0419	0.0225	0.0364	0.0376
8	0.340	0.490	0.0816	0.0390	0.0395	0.0226	0.0271	0.0299
9	0.325	0.366	0.0816	0.0377	0.0414	0.0222	0.0330	0.0264
10	0.328	0.343	0.0852	0.0372	0.0876	0.0197	0.0316	0.0323
11	0.330	0.384	0.0885	0.0350	0.0370	0.0216	0.0300	0.0277
12	0.332	0.336	0.165	0.0373	0.0343	0.0215	0.0262	0.0292
13	0.333	0.365	0.0986	0.0360	0.0341	0.0222	0.0283	0.0277
14	0.331	0.349	0.0903	0.0372	0.0414	0.0188	0.0394	0.0372
15	0.327	0.500	0.124	0.0362	0.0428	0.0194	0.0369	0.0277
16	0.330	0.337	0.113	0.0384	0.0486	0.0375	0.0323	0.0338
17	0.328	0.337	~	~	~	~	~	~
18	0.318	0.401	~	~	~	~	~	~
19	0.328	0.342	~	~	~	~	~	~
20	0.329	0.344	~	~	~	~	~	~
21	0.320	0.342	~	~	~	~	~	~
22	0.338	0.385	~	~	~	~	~	~
23	0.339	0.358	~	~	~	~	~	~
24	0.336	0.426	~	~	~	~	~	~
25	0.333	0.365	~	~	~	~	~	~
26	0.345	0.376	~	~	~	~	~	~
27	0.332	0.378	~	~	~	~	~	~
28	0.340	0.367	~	~	~	~	~	~
29	0.331	0.426	~	~	~	~	~	~
30	0.342	0.377	~	~	~	~	~	~
31	0.344	0.383	~	~	~	~	~	~
32	0.345	0.393	~	~	~	~	~	~

Table 8: Cold Plateau (28V) NEdT at L_{typ} for each band and detector (HAM side A).

Detector	I4	I5	M12	M13 hg	M14	M15	M16A	M16B
1	0.433	0.341	0.0822	0.0362	0.0361	0.0221	0.0370	0.0305
2	0.440	0.390	0.0789	0.0351	0.0395	0.0186	0.0319	0.0311
3	0.434	0.345	0.0814	0.0356	0.0402	0.0159	0.0273	0.0332
4	0.431	0.353	0.0822	0.0421	0.0403	0.0179	0.0365	0.0349
5	0.425	0.386	0.0814	0.0343	0.0461	0.0153	0.0267	0.0299
6	0.424	0.472	0.0817	0.0382	0.0364	0.0195	0.0299	0.0373
7	0.420	0.369	0.0793	0.0357	0.0412	0.0222	0.0273	0.0315
8	0.421	0.523	0.0799	0.0376	0.0393	0.0216	0.0277	0.0319
9	0.408	0.363	0.0809	0.0352	0.0421	0.0216	0.0314	0.0293
10	0.409	0.351	0.0827	0.0359	0.0901	0.0238	0.0329	0.0406
11	0.414	0.378	0.0876	0.0366	0.0371	0.0248	0.0342	0.0316
12	0.413	0.332	0.160	0.0375	0.0345	0.0224	0.0328	0.0307
13	0.414	0.359	0.0981	0.0359	0.0341	0.0204	0.0310	0.0317
14	0.410	0.353	0.0901	0.0393	0.0418	0.0143	0.0355	0.0376
15	0.409	0.470	0.124	0.0374	0.0437	0.0218	0.0304	0.0275
16	0.414	0.337	0.113	0.0382	0.0471	0.0230	0.0354	0.0311
17	0.410	0.339	~	~	~	~	~	~
18	0.401	0.404	~	~	~	~	~	~
19	0.408	0.344	~	~	~	~	~	~
20	0.409	0.348	~	~	~	~	~	~
21	0.409	0.345	~	~	~	~	~	~
22	0.423	0.387	~	~	~	~	~	~
23	0.424	0.365	~	~	~	~	~	~
24	0.420	0.414	~	~	~	~	~	~
25	0.420	0.360	~	~	~	~	~	~
26	0.428	0.379	~	~	~	~	~	~
27	0.416	0.396	~	~	~	~	~	~
28	0.423	0.361	~	~	~	~	~	~
29	0.418	0.466	~	~	~	~	~	~
30	0.425	0.391	~	~	~	~	~	~
31	0.432	0.377	~	~	~	~	~	~
32	0.425	0.392	~	~	~	~	~	~

Table 9: Cold Plateau (34V) NEdT at L_{typ} for each band and detector (HAM side A).

Detector	I4	I5	M12	M13 hg	M14	M15	M16A	M16B
1	0.351	0.339	0.0836	0.0388	0.0365	0.0215	0.0392	0.0320
2	0.361	0.386	0.0802	0.0349	0.0388	0.0213	0.0329	0.0324
3	0.354	0.334	0.0780	0.0374	0.0389	0.0196	0.0300	0.0328
4	0.353	0.357	0.0826	0.0444	0.0399	0.0239	0.0365	0.0335
5	0.348	0.375	0.0809	0.0368	0.0460	0.0237	0.0292	0.0333
6	0.342	0.491	0.0840	0.0352	0.0345	0.0190	0.0293	0.0348
7	0.334	0.368	0.0808	0.0351	0.0410	0.0198	0.0369	0.0270
8	0.348	0.449	0.0794	0.0381	0.0388	0.0190	0.0296	0.0287
9	0.328	0.385	0.0823	0.0374	0.0398	0.0249	0.0319	0.0338
10	0.328	0.351	0.0824	0.0370	0.0923	0.0213	0.0335	0.0343
11	0.336	0.390	0.0897	0.0362	0.0357	0.0250	0.0342	0.0326
12	0.334	0.339	0.164	0.0357	0.0349	0.0185	0.0284	0.0337
13	0.328	0.367	0.0977	0.0369	0.0359	0.0174	0.0286	0.0340
14	0.331	0.355	0.0846	0.0410	0.0414	0.0191	0.0378	0.0343
15	0.330	0.498	0.123	0.0365	0.0442	0.0257	0.0319	0.0290
16	0.335	0.338	0.114	0.0414	0.0477	0.0169	0.0302	0.0350
17	0.328	0.342	~	~	~	~	~	~
18	0.320	0.396	~	~	~	~	~	~
19	0.330	0.336	~	~	~	~	~	~
20	0.333	0.349	~	~	~	~	~	~
21	0.326	0.351	~	~	~	~	~	~
22	0.342	0.383	~	~	~	~	~	~
23	0.341	0.353	~	~	~	~	~	~
24	0.338	0.425	~	~	~	~	~	~
25	0.337	0.358	~	~	~	~	~	~
26	0.348	0.378	~	~	~	~	~	~
27	0.332	0.377	~	~	~	~	~	~
28	0.343	0.365	~	~	~	~	~	~
29	0.334	0.480	~	~	~	~	~	~
30	0.345	0.377	~	~	~	~	~	~
31	0.349	0.387	~	~	~	~	~	~
32	0.347	0.384	~	~	~	~	~	~

Figure 1: Cold Plateau (22V) SNR versus background subtracted source radiance for bands I4, I5, M12, and M13 hg with fractional fitting residuals.

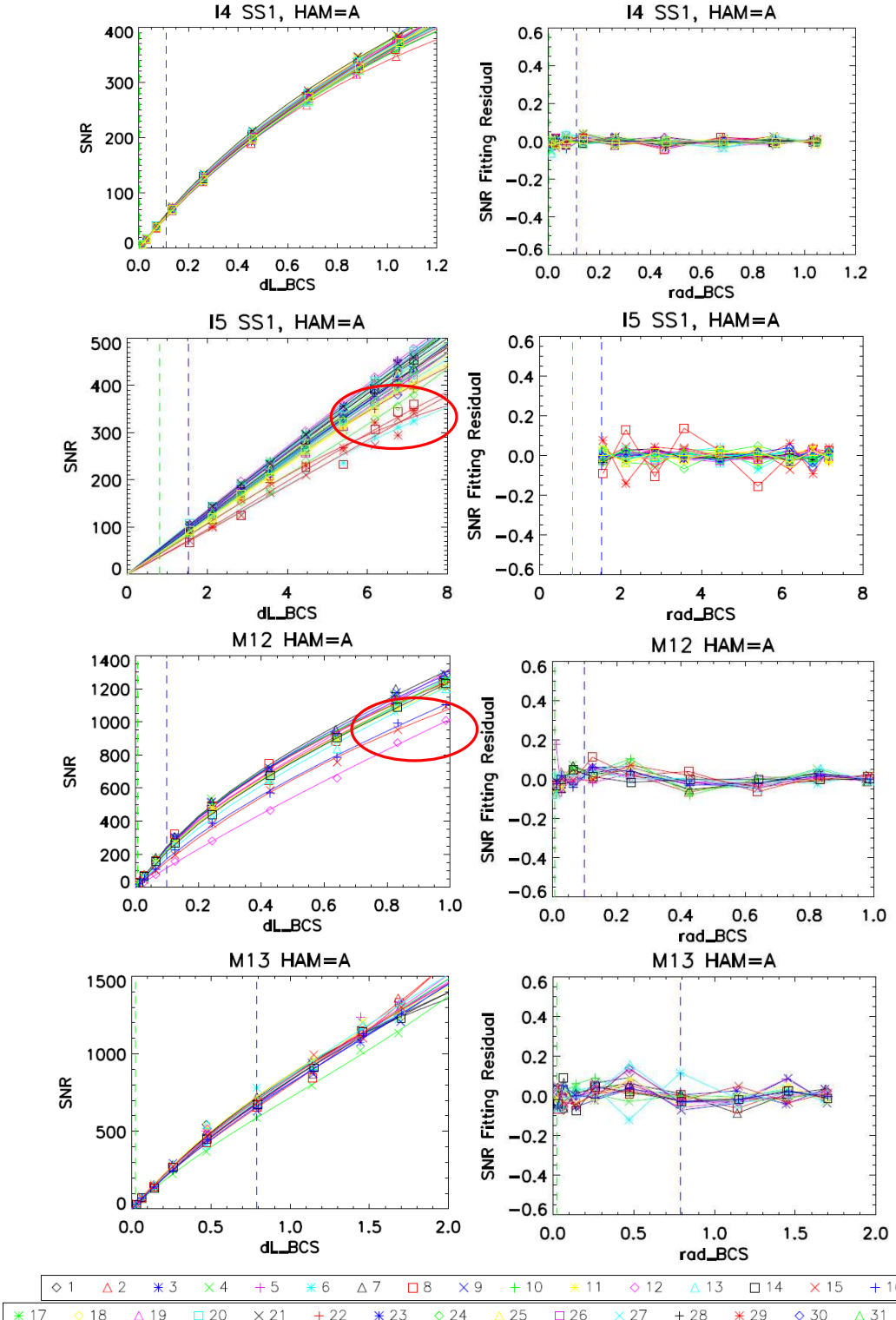


Figure 2: Cold Plateau (22V) SNR versus background subtracted source radiance for bands M14, M15, M16A, and M16B with fractional fitting residuals.

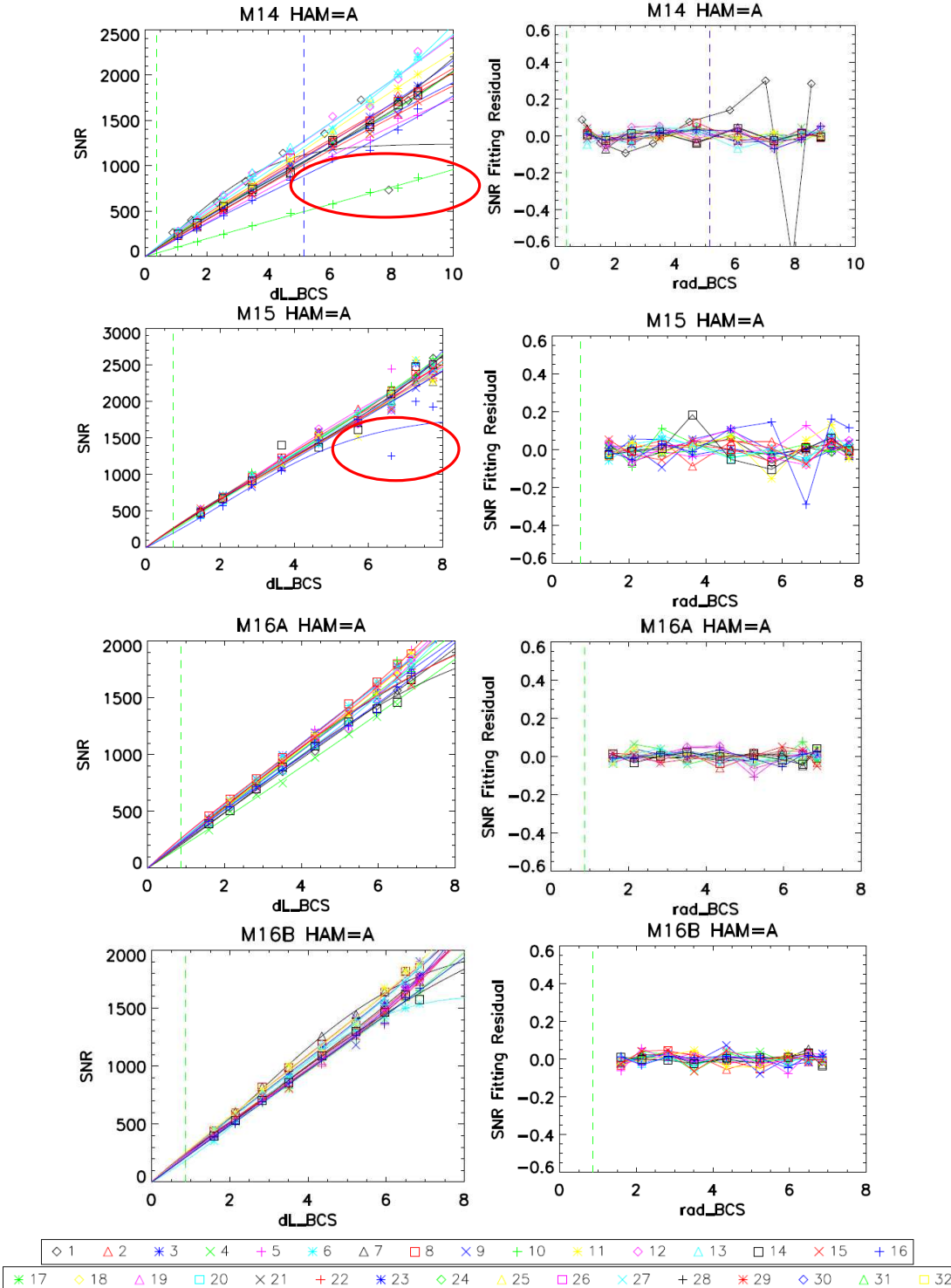


Figure 3: Cold Plateau (28V) SNR versus background subtracted source radiance for bands I4, I5, M12, and M13 hg with fractional fitting residuals.

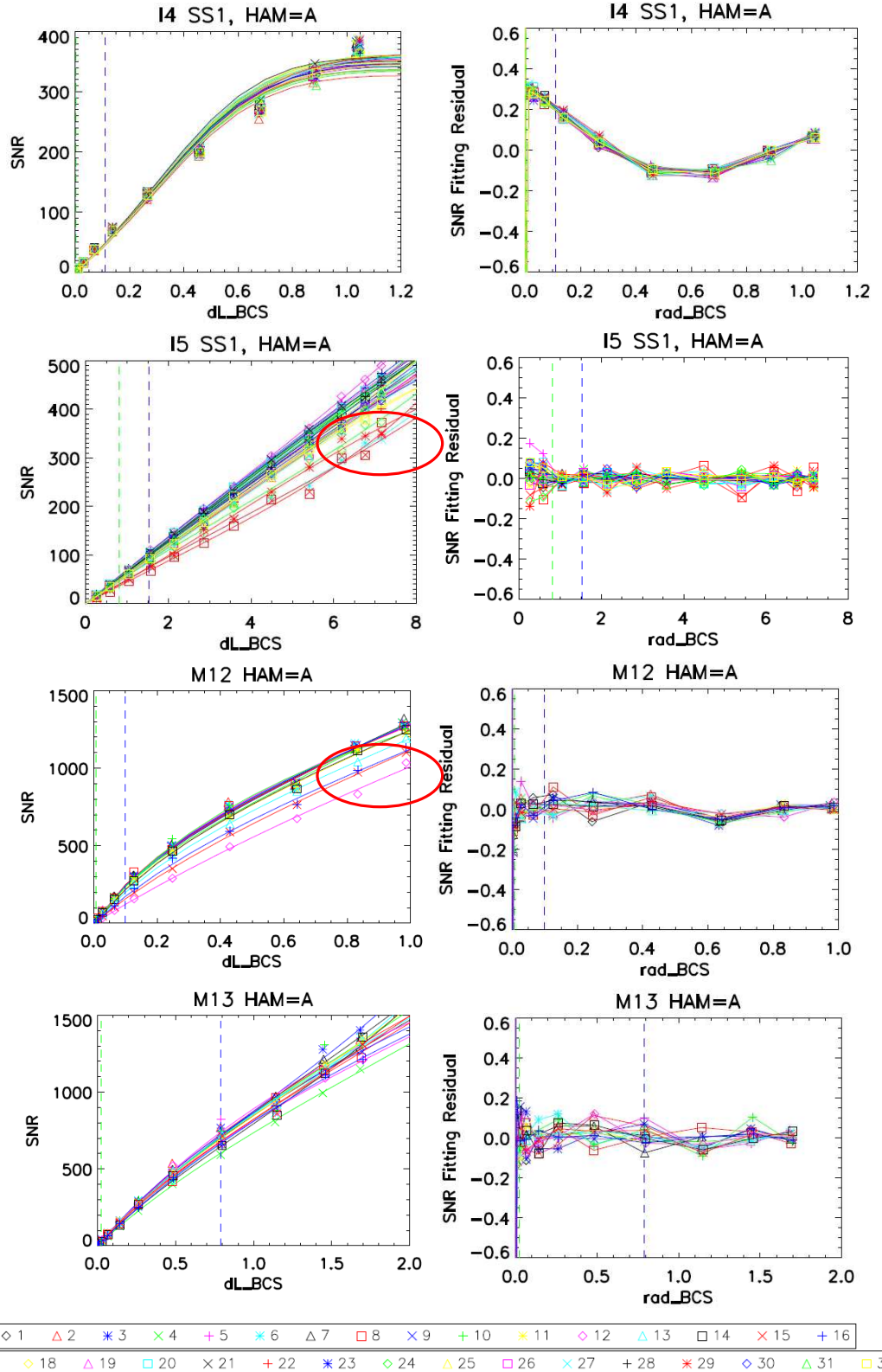


Figure 4: Cold Plateau (28V) SNR versus background subtracted source radiance for bands M14, M15, M16A, and M16B with fractional fitting residuals.

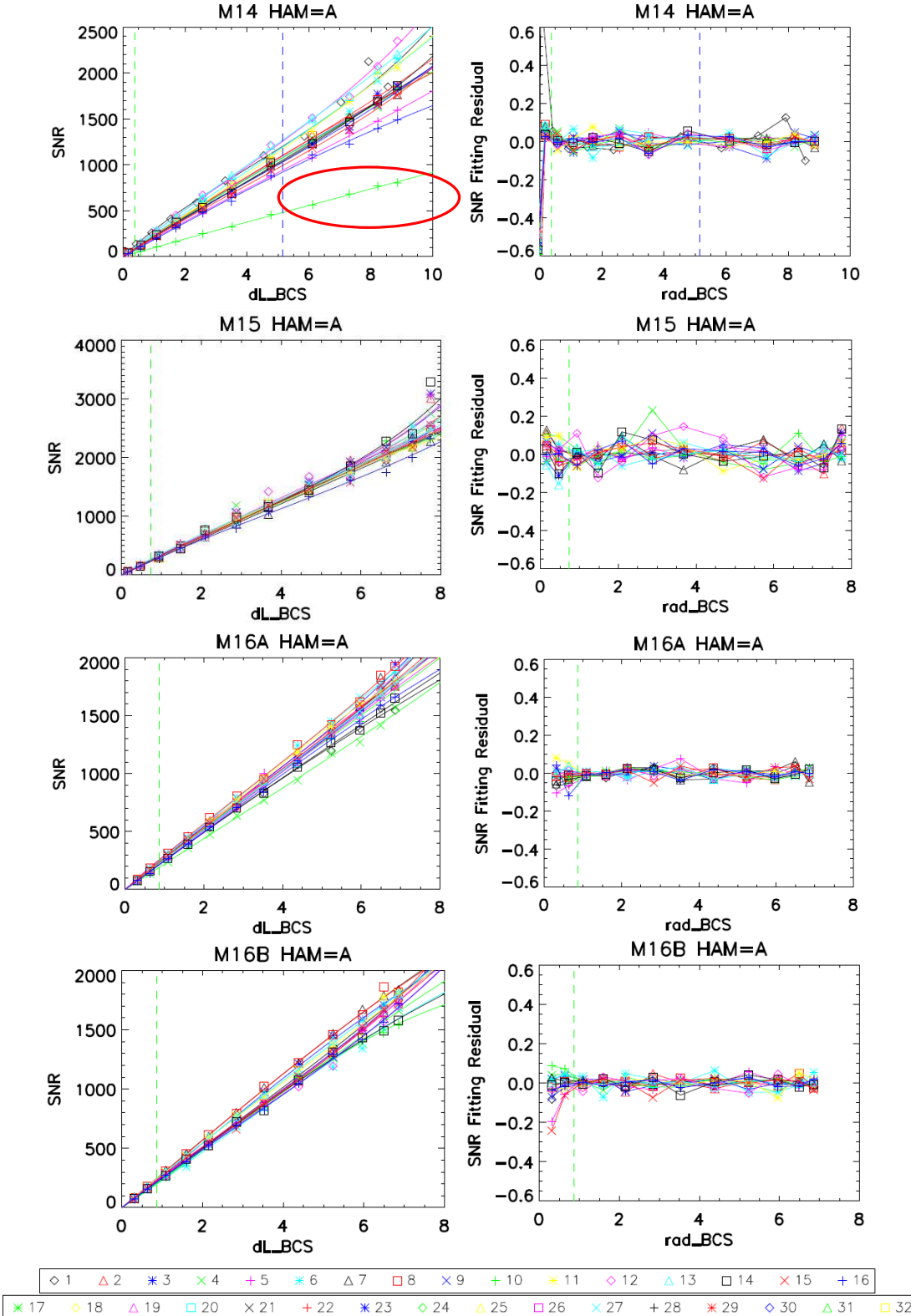


Figure 5: Cold Plateau (34V) SNR versus background subtracted source radiance for bands I4, I5, M12, and M13 hg with fractional fitting residuals.

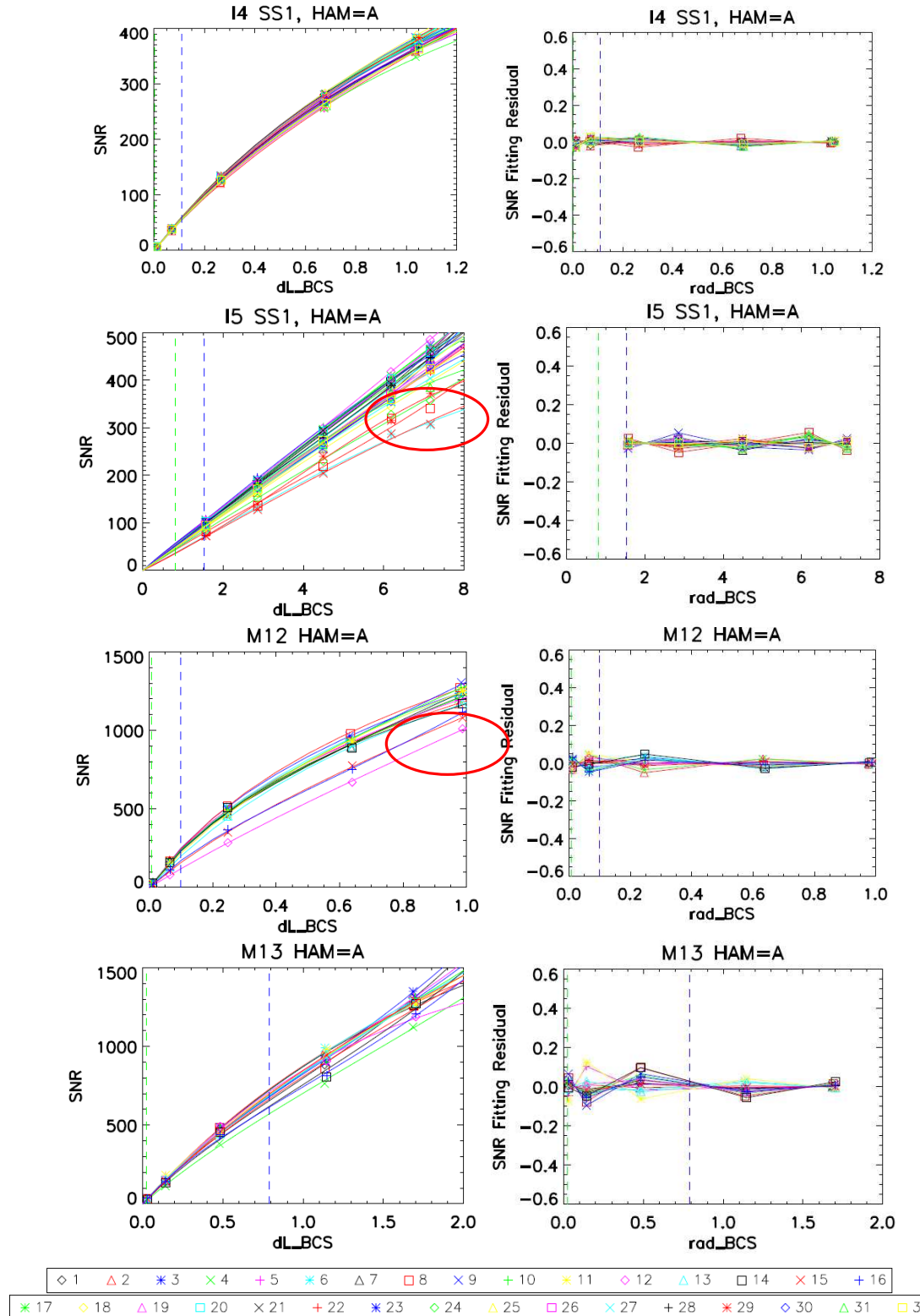


Figure 6: Cold Plateau (34V) SNR versus background subtracted source radiance for bands M14, M15, M16A, and M16B with fractional fitting residuals.

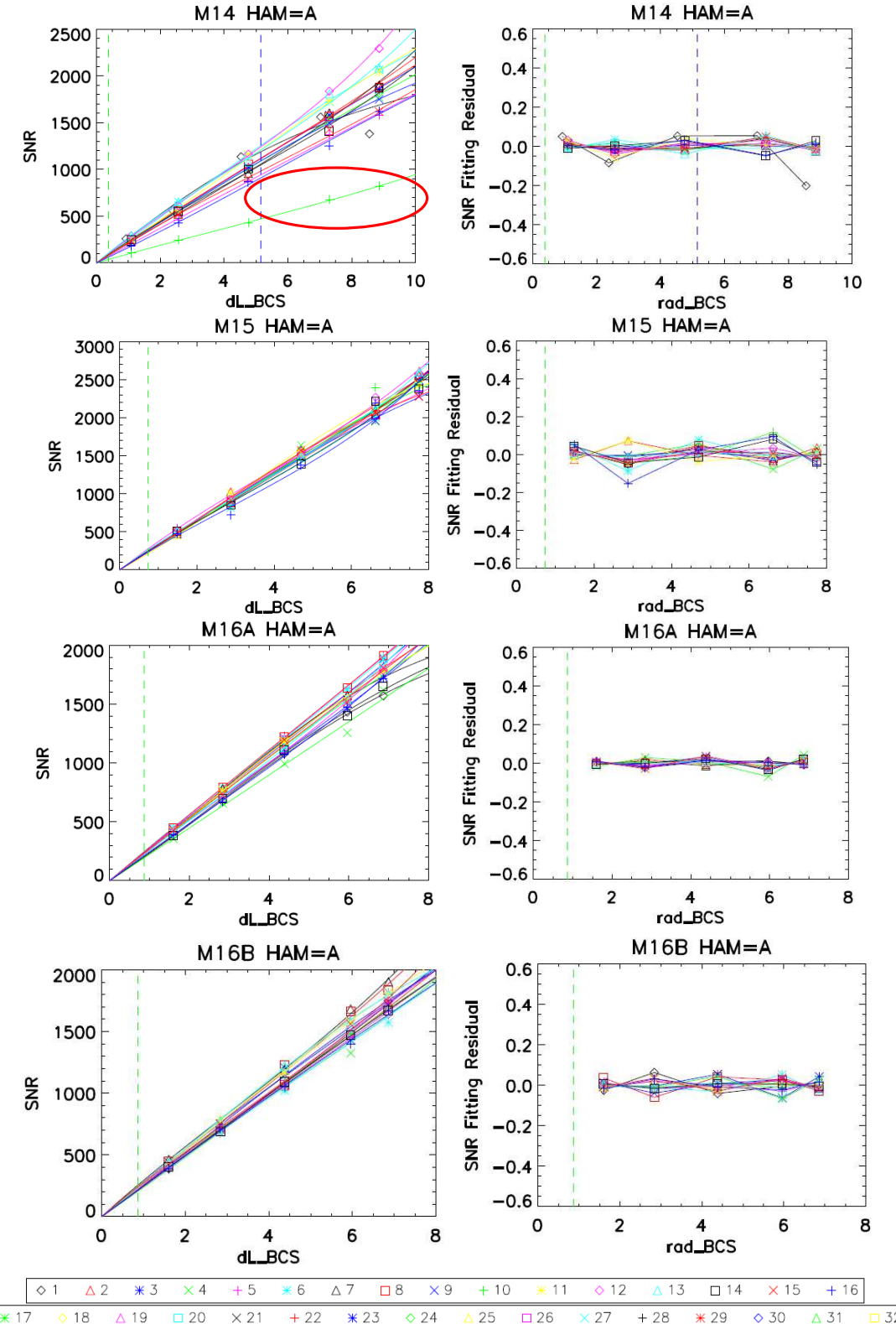


Figure 7: Cold Plateau (22V) SNR at L_{Typ} for all bands as a function of detector.

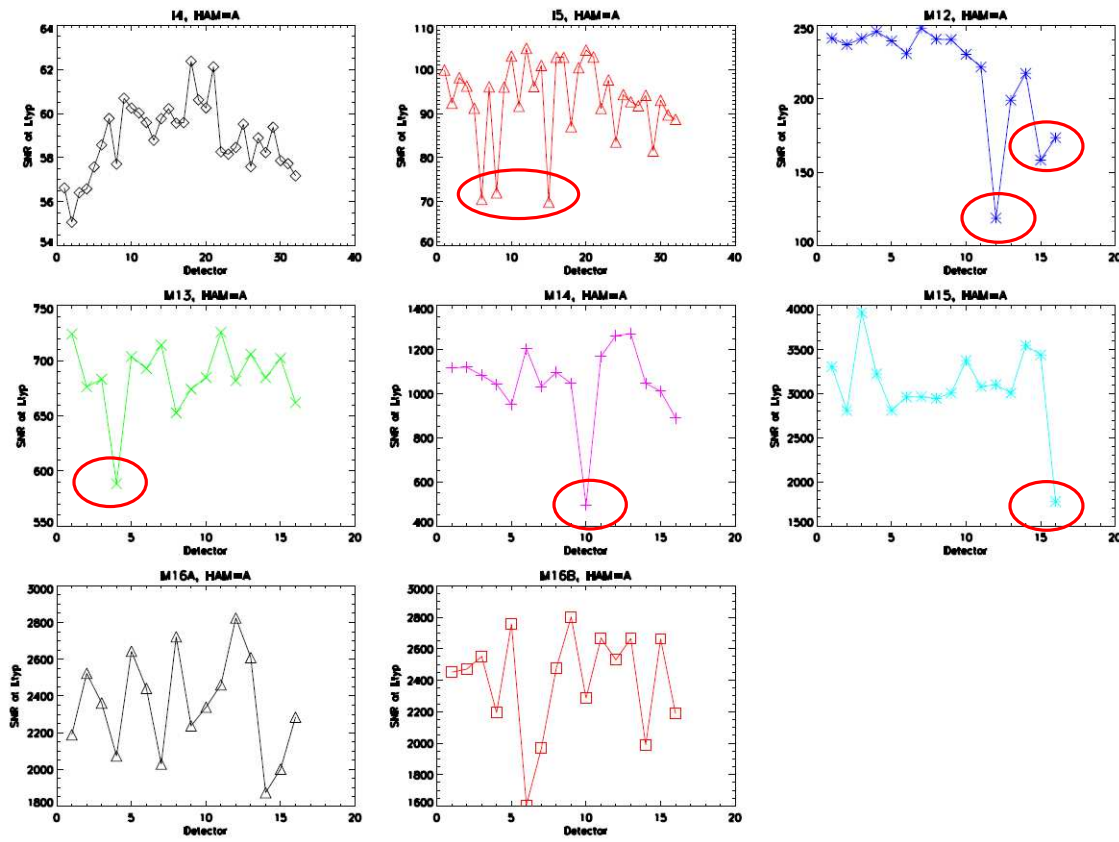


Figure 8: Cold Plateau (28V) SNR at L_{Typ} for all bands as a function of detector.

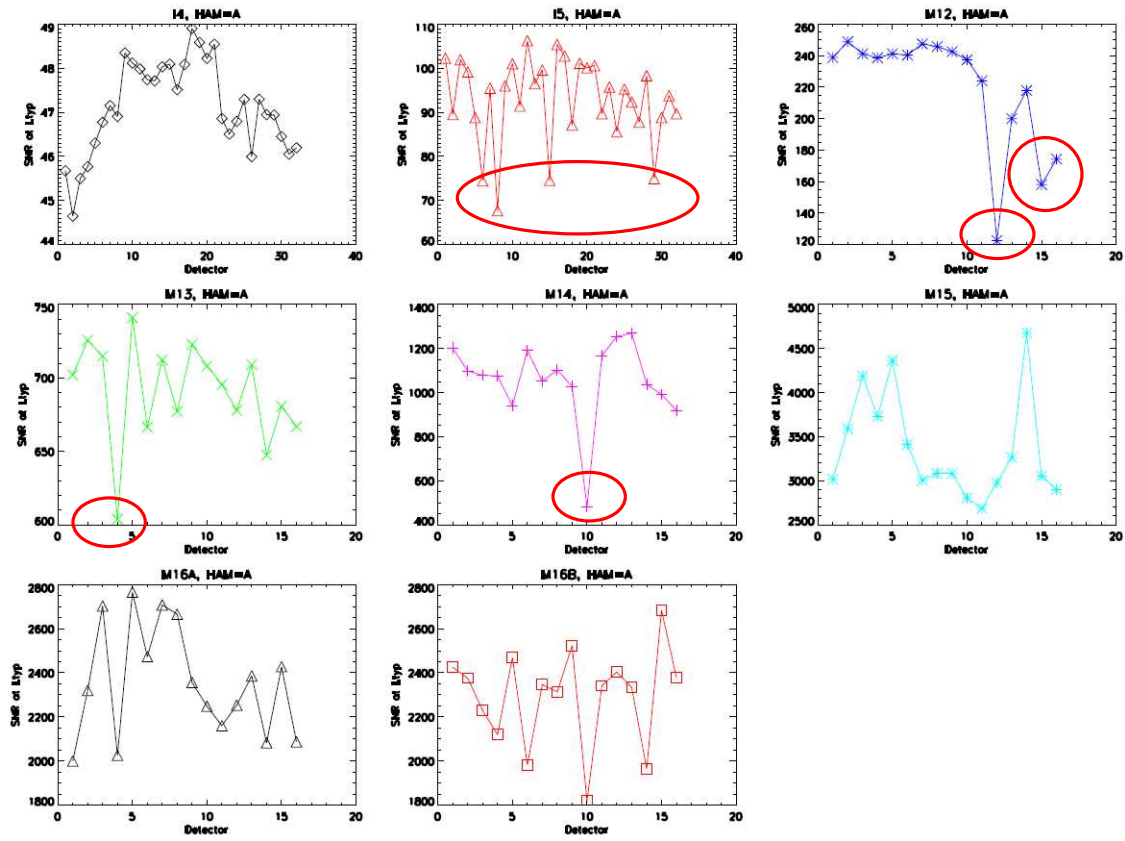


Figure 9: Cold Plateau (34V) SNR at L_{Typ} for all bands as a function of detector.

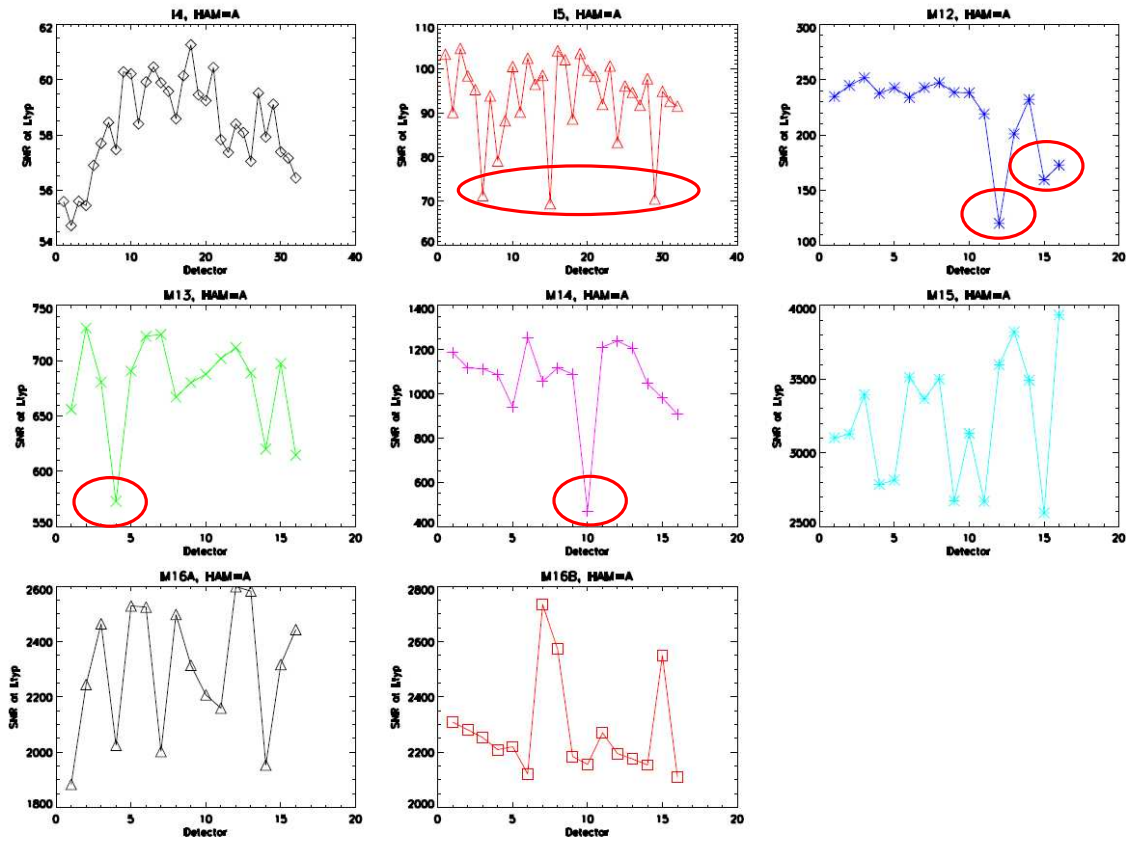


Figure 10: Cold Plateau (22V) NEdT versus dL_BCS for all bands and detectors.

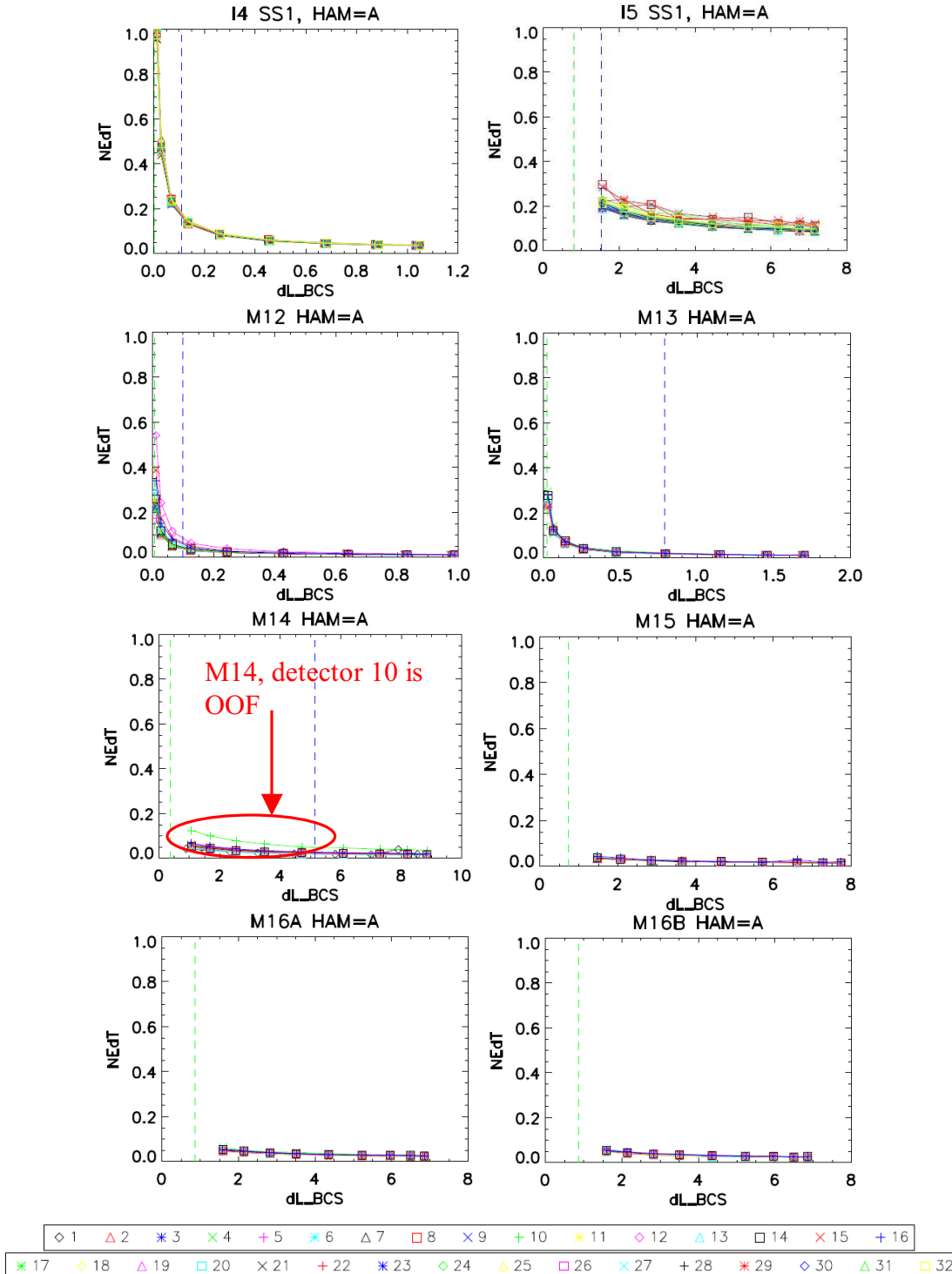


Figure 11: Cold Plateau (28V) NEdT versus dL_BCS for all bands and detectors.

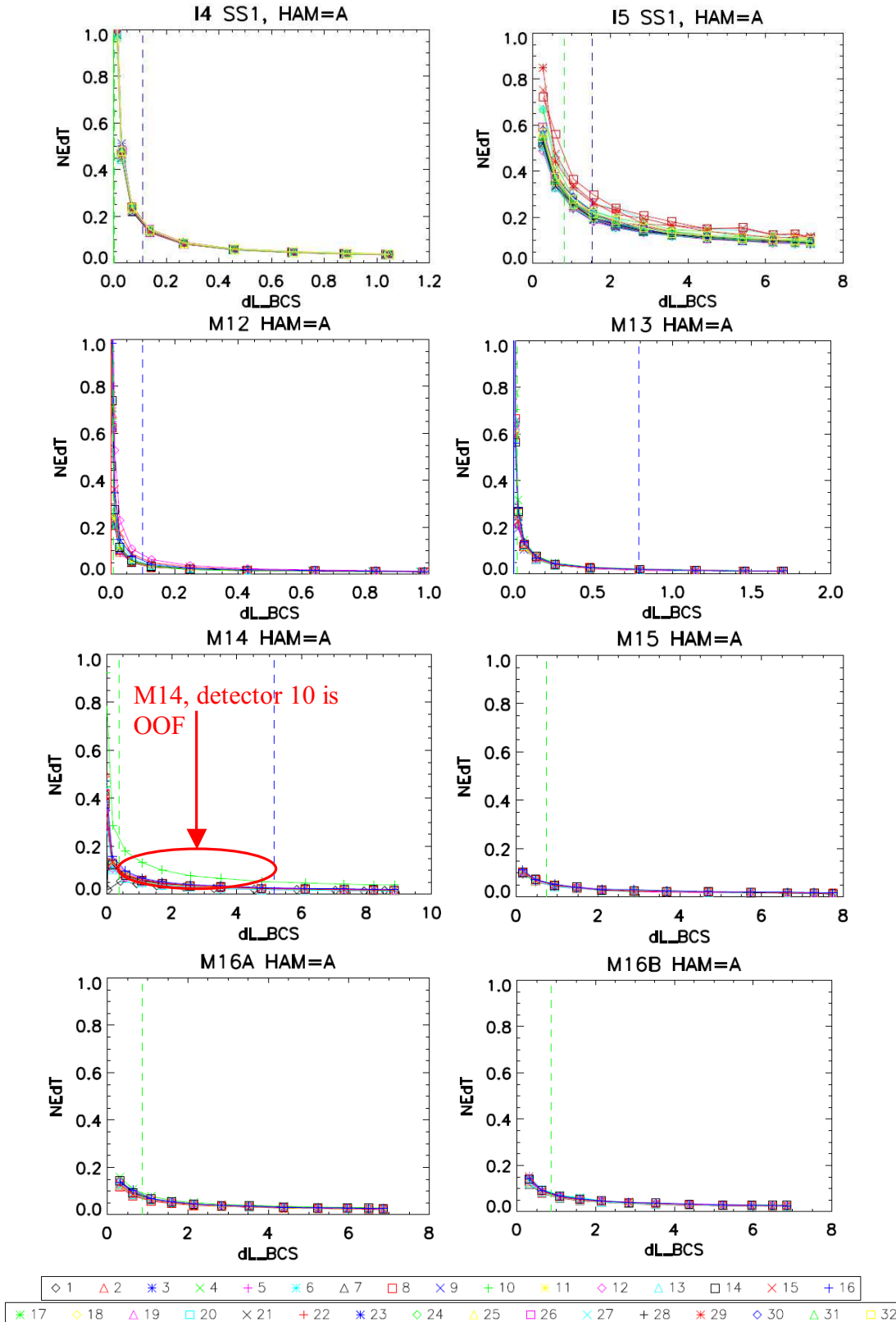


Figure 12: Cold Plateau (34V) NEdT versus dL_BCS for all bands and detectors.

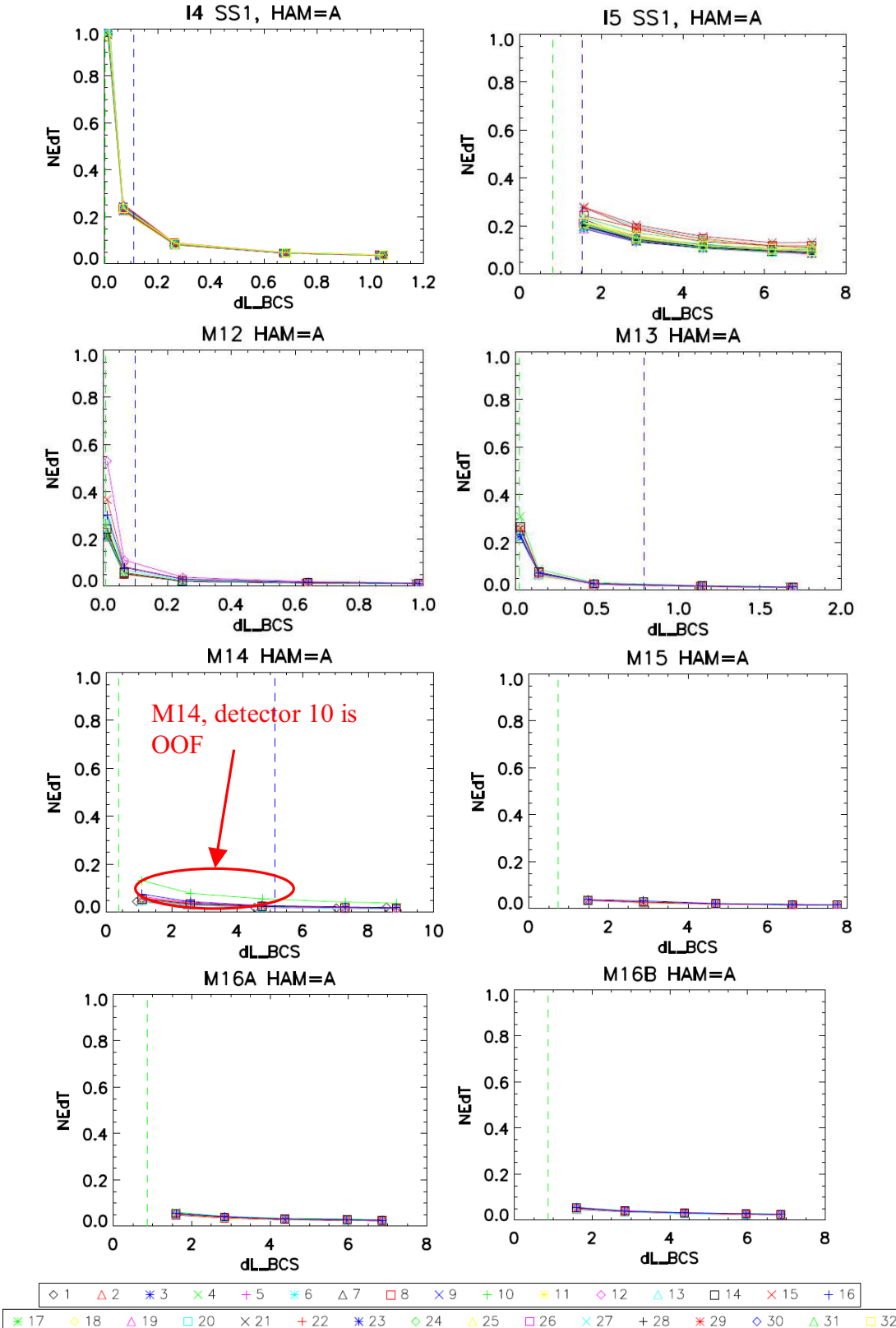


Figure 13: Cold Plateau (22V) NEdT at L_{TYP} for all bands as a function of detector.

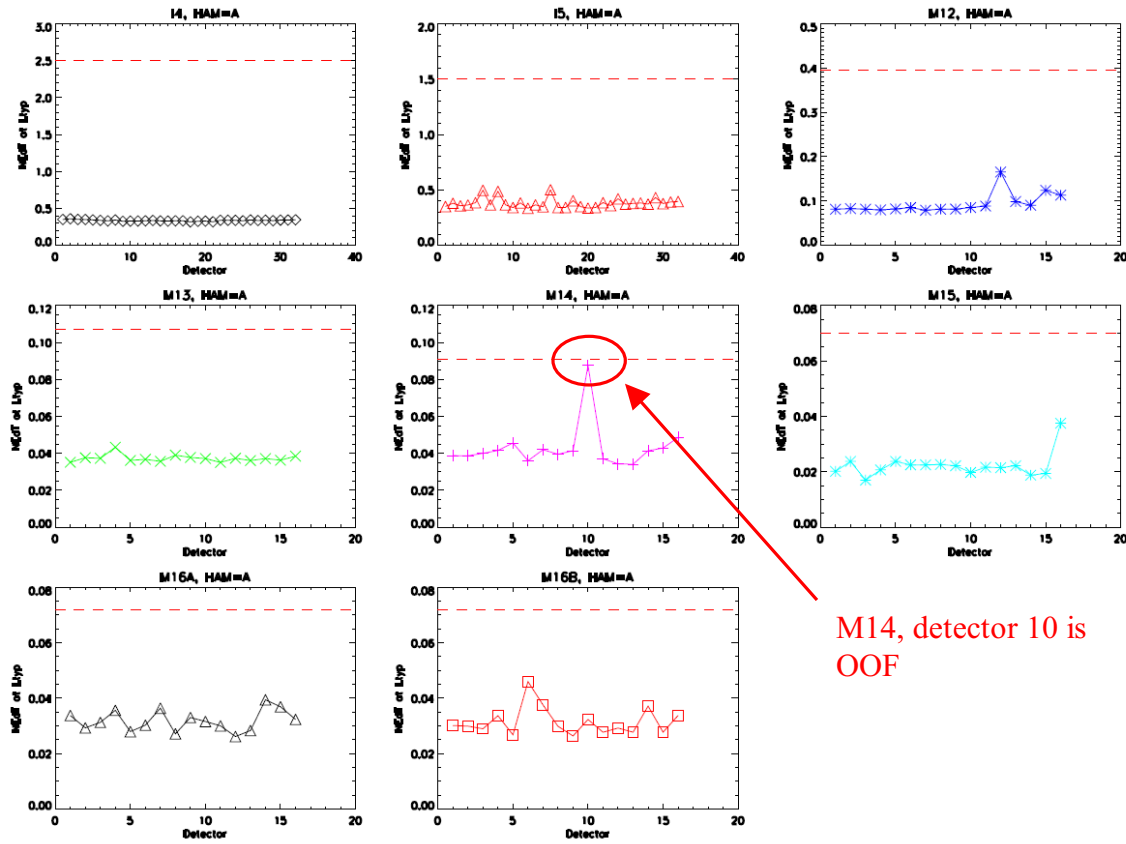
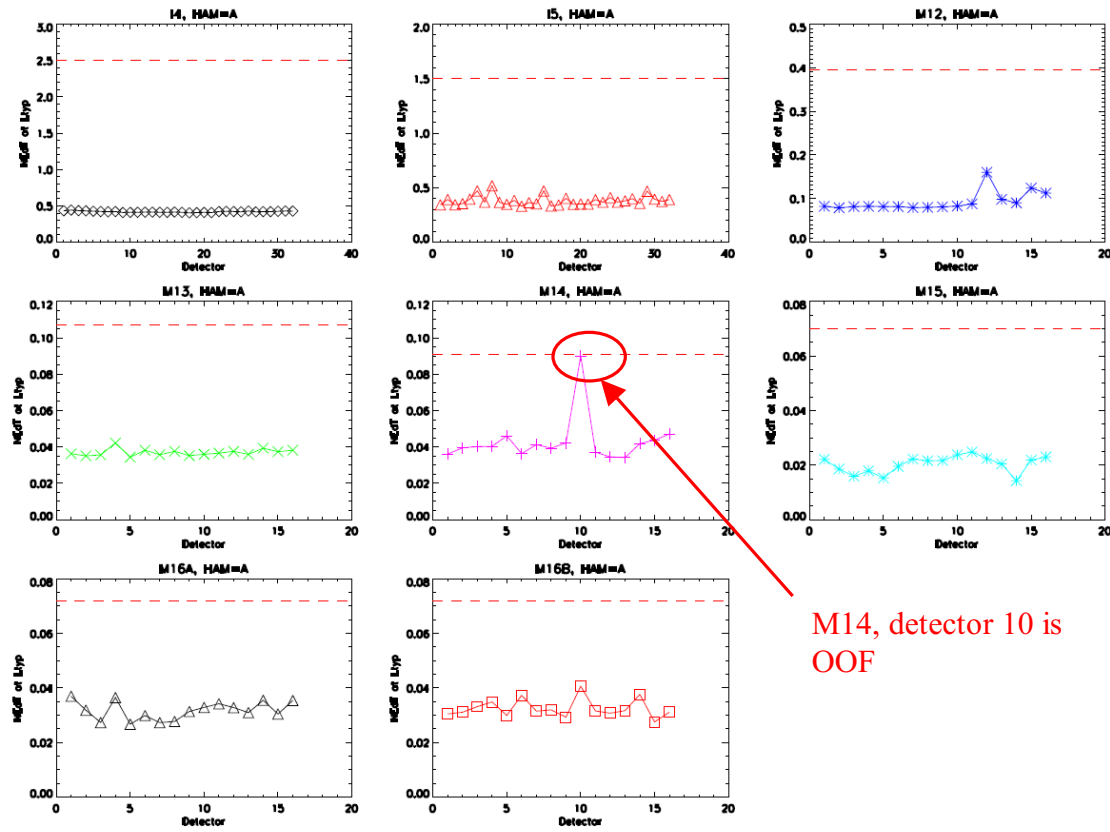


Figure 14: Cold Plateau (28V) NEdT at L_{TYP} for all bands as a function of detector.



M14, detector 10 is
OOF

Figure 15: Cold Plateau (34V) NEdT at L_{TYP} for all bands as a function of detector.

